Nanoscale

COMMUNICATION

View Article Online
View Journal | View Issue

Cite this: *Nanoscale*, 2018, **10**, 12297

Received 31st January 2018,
Accepted 12th June 2018

DOI: 10.1039/c8nr00871j

rsc.li/nanoscale

Breaking the Nd^{3+}-sensitized upconversion nanoparticles myth about the need of onion-layered structures†

Nestor Estebanez,[a] Juan Ferrera-González,[a] Laura Francés-Soriano,[a] Raul Arenal,[b,c] María González-Béjar *[a] and Julia Pérez-Prieto *[a]

Up to now, most strategies to build efficient 800 nm-light responsive upconversion nanoparticles (UCNPs) have included onion-layered structures, in which Nd^{3+} is confined within the inorganic crystal structure of at least one layer. We report here an easy room-temperature modular preparation of core–shell UCNPs consisting of $NaYF_4$:Yb,Er(Tm)/$NaYF_4$ (UC_{CS}) with Nd^{3+} anchored at the organic capping by using cucurbituril[7] (CB[7]) as an adhesive. Strikingly, excitation at 800 nm effectively triggers the upconversion emission of UC_{CS}@CB[7]@Nd nanohybrids.

Lanthanide upconversion nanoparticles (UCNPs) convert near-infrared (NIR) light to shorter wavelengths by means of multiphoton absorption assisted by real electronic excited states.[1] Their good photo(physical) stability, size-independent optical features, narrow emission lines, large anti-Stokes shift and low long-term cytotoxicity make them far superior to other traditionally used emissive nanoparticles (NPs), such as quantum and carbon dots and gold NPs.

Initially, core–shell β-$NaYF_4$:Yb,X/$NaYF_4$ (X = Er, Tm) (UC_{CS}) have been the preferred choice due to their supreme upconversion luminescence (UCL) attributed to their hexagonal crystal structure[1] together with the presence of an inert $NaYF_4$ inorganic shell that reduces the surface quenching effects due to energy migration to the surface.[2] In these UCNPs, Yb absorbs 980 nm light (absorption cross section of $\sim 10^{-20}$ cm^2)[3] and transfers the energy to the activator (*e.g.* Er, Tm). Given that water absorbs at 980 nm, but hardly at all at 800 nm (absorption coefficient 0.48 *vs.* 0.02 cm^{-1}, respectively),[4] Nd^{3+}-doped UCNPs able to upconvert light of ≈800 nm to visible or NIR have been developed over the last decade with a view to minimizing water absorption and its associated heating effects, as well as improving the penetration depth into tissues.[5] Nd^{3+}-sensitized UCL after 800 nm excitation occurs as a result of Nd → Yb → activator (Er/Tm) energy transfer (Scheme S1†) due to the fact that the Nd^{3+} absorption cross-section (1.2×10^{-19} cm^2) is 10 times higher than that of Yb^{3+}.[5c,6]

Thus, Nd^{3+} acts as the primary sensitizer to absorb 800 nm photons, and Yb^{3+} is the bridging sensitizer, which transfers energy to the activator.[5c,7] Unfortunately, Nd^{3+} induces a drastic quenching effect caused by efficient back energy transfer from the activator to Nd^{3+}.[8] The most widely used strategy to build efficient 800 nm-light responsive UCNPs include onion-layered structures.[7b,9] In these structures, Nd^{3+} is confined within the inorganic crystal structure of at least one layer, it is encapsulated in the core and/or the shell in order to facilitate the energy transfer to Yb^{3+}, and it is usually in a different layer from that of the activators (core and/or the shell) in order to facilitate the energy transfer to Yb^{3+}. In addition, architectures in which a sandwiched shell (only doped with Yb^{3+}), between a core doped with Yb^{3+} and the activator ions and an outer shell doped with Nd^{3+} (and sometimes Yb^{3+}) have also been built with the same purpose. An inert and thick outer shell has been considered crucial to overcome concentration quenching effects in lanthanide-doped NPs.[7b,10] There is no doubt that the synthesis of these structures is elaborate, challenging and time-consuming.[6,7,11] A new class of 800 nm-light responsive UCNPs without Nd^{3+} sensitizers is that of Er^{3+}-enriched nanostructures[2c,10,12] (*e.g.*, $NaErF_4$@$NaYF_4$), in which a thick shell mitigates the concentration quenching effect.

Based on the reported low responsiveness of Nd^{3+} luminescence to surface quenching,[7b] and with the aim of preparing Nd^{3+}-sensitized UCNPs by a less challenging procedure than that of onion-layered nanostructures, we planned an alternative, modular synthesis of UCNPs with non-encapsulated Nd^{3+} ions at the NP periphery at a fixed distance from the NP surface. Here we present a new, easy to perform strategy to prepare UCNPs responsive to both 980 nm and 800 nm excitation. It consists of a modular construction based on a set of

[a]*Instituto de Ciencia Molecular (ICMol), University of Valencia, Catedrático José Beltrán 2, 46980 Paterna, Valencia, Spain. E-mail: maria.gonzalez@uv.es, julia.perez@uv.es*
[b]*Laboratorio de Microscopias Avanzadas (LMA), Instituto de Nanociencia de Aragon (INA), U. Zaragoza, 50018 Zaragoza, Spain*
[c]*ARAID Foundation, 50018 Zaragoza, Spain*

† Electronic supplementary information (ESI) available: Experimental data, EDS, HRTEM, TEM images, XRD, ATR-FTIR, TGA, emission spectra, confocal images and conversion of intensity profile to kinetics. See DOI: 10.1039/c8nr00871j

three components that place Nd^{3+} at *ca.* 1 nm from the surface of a core–shell $NaYF_4$:Yb,X/$NaYF_4$ (X = Er, Tm) NP. Remarkably, we demonstrate here that Nd^{3+}, even if it is not within the nanocrystal lattice, can act as a sensitizer of UCL after its excitation at 800 nm (Fig. 1). This modular design is proposed in the wake of our recent discoveries, which showed not only that core $NaYF_4$:Yb,X (UC_C) NPs can be efficiently capped with rigid cucurbituril hosts (CB[n], n = 5–7)[13] but also that the CB[n] free portal (*i.e.* the portal not interacting with the UC_C surface) can readily bind to cations.[14]

Accordingly, UC_{CS} have been capped with cucurbituril[7] (UC_{CS}@CB) and, subsequently, Nd^{3+} has been added to cap the free CB portal, thus producing UC_{CS}@CB@Nd nanohybrids (Fig. 1). This architecture would mitigate cross-relaxation processes between Nd and the activator, even when using a relatively thin inactive shell and, therefore, under the potential occurrence of ion diffusion during the epitaxial growth process.[15,16]

Firstly, oleate-capped UCNPs, $UC_{CS,Er}$@OA and $UC_{CS,Tm}$@OA, are prepared as previously described and fully characterized.[2a,17] $UC_{CS,Er}$@OA have an average size of 38 ± 2 × 66 ± 3 nm which includes an anisotropic shell of an inert $NaYF_4$ layer of *ca.* 3 × 26 nm. The size of $UC_{CS,Tm}$@OA is 21 ± 1 × 31 ± 2 nm which includes a $NaYF_4$ layer of *ca.* 4 × 7 nm. Secondly, naked UC_{CS} are obtained by acidification of UC_{CS}@OA with HCl.[18] Then, a mixture of CB[7] and naked UC_{CS} is stirred for 48 hours to afford water-dispersible UC_{CS}@CB NPs nanohybrids.[13a]

HRTEM images prove that the shape and size of UC_{CS} remain identical upon addition of CB[7] (see experimental details and Fig. S1–S7 in the ESI†). Fig. 2A, B, D show a thin sheath covering $UC_{CS,Er}$ attributed to CB[7] (see Fig. S3† for $UC_{CS,Tm}$@CB). Finally, UC_{CS}@CB@Nd nanohybrids were prepared by mixing UC_{CS}@CB with an excess of $NdCl_3$ salt.

Indeed, the presence of Nd^{3+} in the thin organic capping is confirmed by energy dispersive X-rays spectroscopy (EDS; see Fig. 2E and Table S1 in the ESI†). The ratio of Nd^{3+} was *ca.* 2 atoms per CB molecule for both $UC_{CS,Er}$@CB@Nd and $UC_{CS,Tm}$@CB@Nd nanohybrids. This suggests the coordination of two Nd^{3+} ions at each CB free portal.[19]

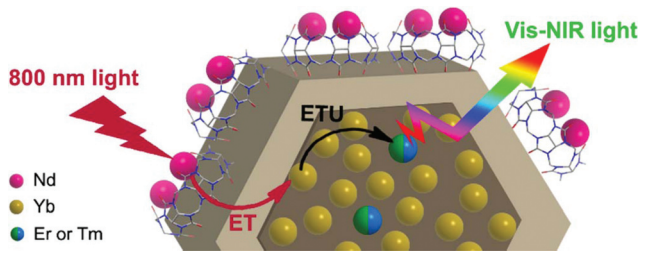

Fig. 1 Schematic representation of a $NaYF_4$:Yb,X/$NaYF_4$ (X = Er, Tm) core–shell NP (UC_{CS}) coated with CB[7] and Nd^{3+} and the processes occurring after 800 nm excitation: Nd^{3+} ions anchored at the outer rigid organic capping (CB[7]) serve as sensitizers and transfer the energy to Yb^{3+} ions; upconversion emission occurs after subsequent energy migration from Yb^{3+} ions to Er^{3+}/Tm^{3+}.

High-angle annular dark-field (HAADF) scanning transmission electron microscopy (STEM) HAADF-HRSTEM is a very appropriate technique for the detection of single atoms.[20] Therefore, it was used to corroborate the presence of Nd^{3+} at the organic capping of $UC_{CS,Er}$@CB@Nd. It is worth noting that no evidence of irradiation damage in this layer was detected during the acquisition of the images. Fig. 2A corresponds to an image of two nanohybrids. As it can be deduced from the HAADF-HRSTEM image (Fig. 2B), these nanohybrids show a high degree of crystallinity and they are covered by an organic shell with a thickness of about 2–3 nm. The HAADF-HRSTEM micrograph shows the presence of heavy atoms embedded in this organic layer; the highlighted circle in the rectangular area depicted in the inset of Fig. 2B shows two bright dots. The intensity profile extracted from the rectangular area of inset Fig. 2B shows two clearly distinguishable peaks, with a full-width at half-maximum close to 2 Å, which correspond to the two bright dots. The dimensions and intensity of the 2 bright dots as compared to that of the organic sheath, allow us to assign them to Nd single atoms embedded in the covering layer of the NPs. It's worth mentioning that the different brightness of these two neighbouring atoms may be caused by their different location, in terms of height, within the layer. In fact, this aspect is related to the focus conditions and the depth of field.[20c–e]

The UCL spectra (λ_{ex} = 980 nm) of $UC_{CS,Er}$@CB and $UC_{CS,Er}$@CB@Nd exhibit the Er^{3+} characteristic emission bands at *ca.* 550 nm ($4S_{3/2} \rightarrow 4I_{15/2}$) with a small shoulder at 520 nm ($2H_{11/2}$, $4S_{3/2} \rightarrow 4I_{15/2}$) and another band centred at 670 nm ($4F_{9/2} \rightarrow 4I_{15/2}$) (see Fig. 2 for $UC_{CS,Er}$@CB@Nd; spectrum of $UC_{CS,Er}$@CB is similar, not shown); see Fig. S8† for $UC_{CS,Tm}$@CB and $UC_{CS,Tm}$@CB@Nd.[1b]

A laser scanning confocal equipment was used to determine the performance of the UC_{CS}@CB@Nd NPs using short dwell times after NIR excitation, at both 800 nm and 980 nm. This makes it possible not only to study the occurrence of energy transfer processes in the UC_{CS}@CB@Nd nanohybrids but it has also proved to be a useful tool to evaluate luminescence lifetime in a range of several tens of microseconds (see ESI†).[21]

Therefore, samples were prepared by drop-casting a water dispersion of the corresponding NPs onto a 25 × 75 mm microscope glass slide. Then, solvent was evaporated and the sample was covered with a 22 × 22 mm glass slide.

The 515–560 nm channel was used to follow the emissive behavior of $UC_{CS,Er}$@CB@Nd and, for comparative purposes, $UC_{CS,Er}$@CB, taking into account that the emission of these NPs is the strongest in this channel (Fig. 2J). As expected, confocal images of $UC_{CS,Er}$@CB@Nd and $UC_{CS,Er}$@CB at λ_{ex} = 980 nm showed the green emission of the NPs (Fig. 2F and G). The emission quantum yield upon 980 nm excitation of UC_{CS}@CB[7]@Nd and UC_{CS}@CB[7] was measured by using a Quantaurus-QY Plus UV-NIR absolute quantum yield spectrometer (further details in ESI†). UC_{CS}@CB[7] exhibited a higher emission efficiency than the Nd-caped UCNP (1% *vs.* 0.6%,

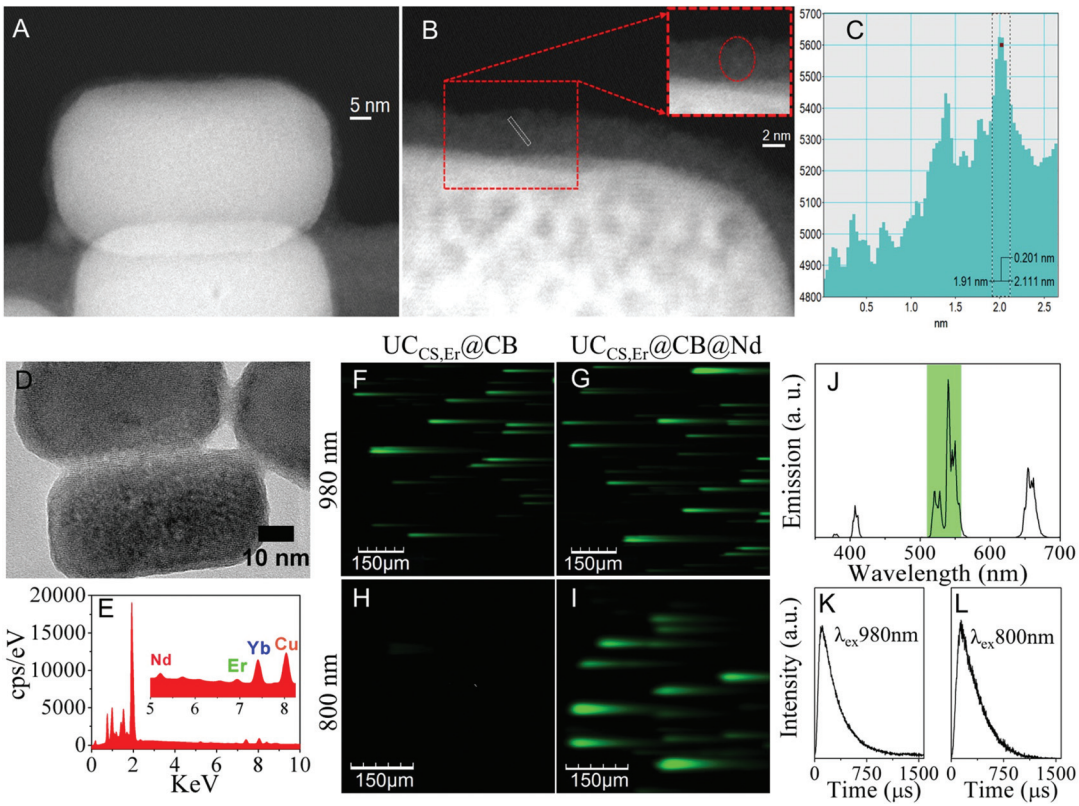

Fig. 2 (A) HAADF-STEM micrograph of two superposed $UC_{CS,Er}$@CB@Nd NPs partially deposited on the carbon support film; in both of them, though it is more evident in the one on top, a thin organic layer is visible; (B) high-resolution HAADF-STEM image of another $UC_{CS,Er}$@CB@Nd NP also covered by a 2–3 nm shell; in the shell, two bright dots can be seen in the highlighted rectangular area (inset at the top); these dots can be identified as Nd single atoms in the NP organic layer; (C) an intensity profile has been obtained on them. These dots can be identified as Nd single atoms embedded in this covering layer of the NPs; (D) HRTEM image and (E) EDS analysis of $UC_{CS,Er}$@CB@Nd nanohybrids; (F,G,H,I) confocal images of $UC_{CS,Er}$@CB@Nd and $UC_{CS,Er}$@CB at λ_{ex} = 980 nm and λ_{ex} = 800 nm (515–560 nm, 2 μs per pixel); (J) emission spectrum at λ_{ex} = 980 nm of a 0.3 mg mL^{-1} dispersion of $UC_{CS,Er}$@CB@Nd in MilliQ water; (K,L) intensity profile of UC_{CS}@CB@Nd NPs obtained from the trace of the emission showed by an aggregate after excitation at (K) 980 nm and (L) 800 nm a dwell time of 2 μs per pixel.

respectively). This is consistent with energy transfer from Yb to Nd.

Then, the images were registered at λ_{ex} = 800 nm to demonstrate the occurrence of Nd → Yb → Er energy transfer in the $UC_{CS,Er}$@CB@Nd UCNP (Fig. 2H and I). Likewise, excitation at 785 nm of UC_{CS},Er@CB and UC_{CS},Er@CB@Nd under the same optical setup (0.497 μm per pixel; 2.0 μs per pixel) evidenced the Nd → Yb → Er energy transfer (Fig. S9†).

The Er emission quantum yield upon 808 nm excitation of UC_{CS}@CB[7]@Nd was 0.001%. This corroborated that the energy transfer from Nd to Yb occurred despite of the inactive shell.

To our knowledge, there are no conventional onion-layered structures to compare our nanohybrid with, *i.e.*, there are no papers reporting on the efficiency of onion-layered UCNPs with the Nd-doped shell separated from the core doped with the Yb,activator ions by the inactive $NaYF_4$ matrix. It is clear that there is room for increasing the efficiency of $NaYF_4$:Yb, Er@$NaYF_4$@CB@Nd by using an active shell (*e.g.*, $NaYbF_4$) instead of un-doped $NaYF_4$.

Finally, Fig. 2K and L show the intensity profiles of $UC_{CS,Er}$@CB@Nd NPs obtained from the trace of the emission exhibited by an aggregate after excitation at 980 nm and 800 nm at a dwell time of 2 μs per pixel (Fig. S10†). The UCL decay lifetimes of the green emission at λ_{ex} = 980 nm were of 245 ± 7 μs and 240 ± 4 μs for $UC_{CS,Er}$@CB and $UC_{CS,Er}$@CB@Nd, respectively. The value was similar for the $UC_{CS,Er}$@CB@Nd photoluminescence decay at λ_{ex} = 800 nm (227 ± 6 μs). Fig. S11–18† illustrate the confocal images for each sample and channel.

Last but not least, these UC_{CS}@CB@Nd nanohybrids could also be used for NIR-to-NIR down conversion fluorescence imaging by following the emission of Nd at about 900, 1060, and 1340 nm.

Conclusions

In summary, we report here an easy modular strategy for preparing UCNPs comprising $NaYF_4$:Yb,Er (Tm)/$NaYF_4$/Nd in

which Nd^{3+} is not located in the crystal structure of the UC_{CS}, but in its organic capping ligand at about 1 nm from the NP surface. Interestingly, the emission of the NP can be triggered after 800 nm excitation. To our knowledge, this is not only the first example of a lanthanide photosensitizer in the organic capping of an UCNP, but it is also the first that demonstrates that Nd^{3+} is able to photosensitize the upconversion process even when it is not encapsulated in an inorganic matrix.

This study is a proof-of-concept, but we anticipate that these architectures will open up new opportunities for constructing novel UCNPs. The easy preparation of these nanosystems will stimulate new areas of research relevant to human health.

Conflicts of interest

The manuscript was written through contributions of all authors. All authors have given approval to the final version of the manuscript. There are no conflicts to declare.

Acknowledgements

We thank MINECO (CTQ2017-82711-P), partially co-financed with FEDER funds; MAT2016-79776-P, Maria de Maeztu: MDM-2015-0538; RTC-2016-5114-5, FPU (LSF, JFG), contract (NEB); RyC (MGB) and Fundación Ramón Areces for financing this research. RA also acknowledges Government of Aragon and ESF under the project "Construyendo Europa desde Aragon" 2014–2020 (grant number E/26). TEM measurements were performed in SCSIE (University of Valencia) or Laboratorio de Microscopias Avanzadas (Instituto de Nanociencia de Aragon-University of Zaragoza). Hamamatsu is also acknowledged for kindly providing a Quantaurus-QY Plus UV-NIR absolute quantum yield spectrometer (C13534-11).

Notes and references

1 (*a*) Z. Gu, L. Yan, G. Tian, S. Li, Z. Chai and Y. Zhao, *Adv. Mater.*, 2013, **25**, 3758; (*b*) X. Li, F. Zhang and D. Zhao, *Chem. Soc. Rev.*, 2015, **44**, 1346; (*c*) W. Xu, X. Chen and H. Song, *Nano Today*, 2017, **17**, 54; (*d*) S. Han, R. Deng, X. Xie and X. Liu, *Angew. Chem., Int. Ed.*, 2014, **53**, 11702; (*e*) Z. Yin, H. Li, W. Xu, S. Cui, D. Zhou, X. Chen, Y. Zhu, G. Qin and H. Song, *Adv. Mater.*, 2016, **28**, 2518.

2 (*a*) N. Francolon, D. Boyer, F. Leccia, E. Jouberton, A. Walter, C. Bordeianu, A. Parat, D. Felder-Flesch, S. Begin-Colin, E. Miot-Noirault, J. M. Chezal and R. Mahiou, *Nanomedicine*, 2016, **12**, 2107; (*b*) M. Y. Hossan, A. Hor, Q. Luu, S. J. Smith, P. S. May and M. T. Berry, *J. Phys. Chem. C*, 2017, **121**, 16592; (*c*) N. J. Johnson, S. He, S. Diao, E. M. Chan, H. Dai and A. Almutairi, *J. Am. Chem. Soc.*, 2017, **139**, 3275.

3 M. J. Weber, *Phys. Rev. B: Solid State*, 1971, **4**, 3153.

4 (*a*) S. Singh, R. G. Smith and L. G. Van Uitert, *Phys. Rev. B: Solid State*, 1974, **10**, 2566; (*b*) R. Arppe, I. Hyppänen, N. Perälä, R. Peltomaa, M. Kaiser, C. Würth, S. Christ, U. Resch-Genger, M. Schäferling and T. Soukka, *Nanoscale*, 2015, **7**, 11746; (*c*) Y.-F. Wang, G.-Y. Liu, L.-D. Sun, J.-W. Xiao, J.-C. Zhou and C.-H. Yan, *ACS Nano*, 2013, **7**, 7200.

5 (*a*) E. S. Levy, C. A. Tajon, T. S. Bischof, J. Iafrati, A. Fernandez-Bravo, D. J. Garfield, M. Chamanzar, M. M. Maharbiz, V. S. Sohal, P. J. Schuck, B. E. Cohen and E. M. Chan, *ACS Nano*, 2016, **10**, 8423; (*b*) B. del Rosal, U. Rocha, E. C. Ximendes, E. Martín Rodríguez, D. Jaque and J. G. Solé, *Opt. Mater.*, 2017, **63**, 185; (*c*) J. Shen, G. Chen, A.-M. Vu, W. Fan, O. S. Bilsel, C.-C. Chang and G. Han, *Adv. Opt. Mater.*, 2013, **1**, 644.

6 X. Xie, N. Gao, R. Deng, Q. Sun, Q.-H. Xu and X. Liu, *J. Am. Chem. Soc.*, 2013, **135**, 12608.

7 (*a*) R. Wang and F. Zhang, in *Near-infrared Nanomaterials: Preparation, Bioimaging and Therapy Applications*, ed. F. Zhang, 2016, p. 1; (*b*) X. Xie, Z. Li, Y. Zhang, S. Guo, A. I. Pendharkar, M. Lu, L. Huang, W. Huang and G. Han, *Small*, 2017, **13**, 1602843.

8 (*a*) L. Marciniak, K. Prorok, L. Francés-Soriano, J. Pérez-Prieto and A. Bednarkiewicz, *Nanoscale*, 2016, **8**, 5037; (*b*) E. C. Ximendes, W. Q. Santos, U. Rocha, U. K. Kagola, F. Sanz-Rodríguez, N. Fernández, S. Gouveia-Neto Ada, D. Bravo, A. M. Domingo, B. del Rosal, C. D. Brites, L. D. Carlos, D. Jaque and C. Jacinto, *Nano Lett.*, 2016, **16**, 1695.

9 (*a*) Y. Zhang, Z. Yu, J. Li, Y. Ao, J. Xue, Z. Zeng, X. Yang and T. T. Tan, *ACS Nano*, 2017, **11**, 2846; (*b*) Z. Hou, K. Deng, C. Li, X. Deng, H. Lian, Z. Cheng, D. Jin and J. Lin, *Biomaterials*, 2016, **101**, 32; (*c*) B. Liu, C. Li, P. Yang, Z. Hou and J. Lin, *Adv. Mater.*, 2017, **29**, 1605434.

10 D. Hudry, D. Busko, R. Popescu, D. Gerthsen, A. M. M. Abeykoon, C. Kübel, T. Bergfeldt and B. S. Richards, *Chem. Mater.*, 2017, **29**, 9238.

11 (*a*) Y. Zhong, G. Tian, Z. Gu, Y. Yang, L. Gu, Y. Zhao, Y. Ma and J. Yao, *Adv. Mater.*, 2014, **26**, 2831; (*b*) Q. Zhan, B. Wang, X. Wen and S. He, *Opt. Mater. Express*, 2016, **6**, 1011.

12 (*a*) J. Zuo, Q. Li, B. Xue, C. Li, Y. Chang, Y. Zhang, X. Liu, L. Tu, H. Zhang and X. Kong, *Nanoscale*, 2017, **9**, 7941; (*b*) Q. Chen, X. Xie, B. Huang, L. Liang, S. Han, Z. Yi, Y. Wang, Y. Li, D. Fan, L. Huang and X. Liu, *Angew. Chem., Int. Ed.*, 2017, **56**, 7605.

13 (*a*) L. Francés-Soriano, M. González-Béjar and J. Pérez-Prieto, *Nanoscale*, 2015, **7**, 5140; (*b*) Y. Sun, W. Zhang, B. Wang, X. Xu, J. Chou, O. Shimoni, A. T. Ung and D. Jin, *Chem. Commun.*, 2018, **54**, 3851.

14 H. Tang, D. Fuentealba, Y. H. Ko, N. Selvapalam, K. Kim and C. Bohne, *J. Am. Chem. Soc.*, 2011, **133**, 20623.

15 (*a*) R. Komban, J. P. Klare, B. Voss, J. Nordmann, H. J. Steinhoff and M. Haase, *Angew. Chem., Int. Ed.*, 2012, **51**, 6506; (*b*) H. Dong, L. D. Sun, W. Feng, Y. Gu, F. Li and C. H. Yan, *ACS Nano*, 2017, **11**, 3289; (*c*) B. Chen, D. Peng,

X. Chen, X. Qiao, X. Fan and F. Wang, *Angew. Chem., Int. Ed.*, 2015, **54**, 12788.

16 Optical inert layers of radial thickness over 12 nm have been constructed to avoid energy migration in multidoped, multilayer UCNPs. Reference 15*b*.

17 (*a*) J. Tang, L. Lei, H. Feng, H. Zhang and Y. Han, *J. Fluoresc.*, 2016, **26**, 2237; (*b*) C. Chen, N. Kang, T. Xu, D. Wang, L. Ren and X. Guo, *Nanoscale*, 2015, **7**, 5249; (*c*) S. Wilhelm, M. Kaiser, C. Würth, J. Heiland, C. Carrillo-Carrion, V. Muhr, O. S. Wolfbeis, W. J. Parak, U. Resch-Genger and T. Hirsch, *Nanoscale*, 2015, **7**, 1403; (*d*) Q. Xiao, Y. Ji, Z. Xiao, Y. Zhang, H. Lin and Q. Wang, *Chem. Commun.*, 2013, **49**, 1527.

18 N. Bogdan, F. Vetrone, G. A. Ozin and J. A. Capobianco, *Nano Lett.*, 2011, **11**, 835.

19 (*a*) L.-L. Liang, Y. Zhao, K. Chen, X. Xiao, J. Clegg, Y.-Q. Zhang, Z. Tao, S.-F. Xue, Q.-J. Zhu and G. Wei, *Polymers*, 2013, **5**, 418; (*b*) E. A. Mainicheva, A. A. Tripolskaya, O. A. Gerasko, D. Y. Naumov and V. P. Fedin, *Russ. Chem. Bull.*, 2006, **55**, 1566.

20 (*a*) V. Ortalan, A. Uzun, B. C. Gates and N. D. Browning, *Nat. Nanotechnol.*, 2010, **5**, 843; (*b*) J. Lu, C. Aydin, N. D. Browning and B. C. Gates, *Angew. Chem., Int. Ed.*, 2012, **51**, 5842; (*c*) R. Arenal, K. March, C. P. Ewels, X. Rocquefelte, M. Kociak, A. Loiseau and O. Stephan, *Nano Lett.*, 2014, **14**, 5509; (*d*) A. Mayoral, Y. Sakamoto and I. Diaz, in *Advanced Transmission Electron Microscopy: Applications to Nanomaterials*, ed. F. L. Deepak, A. Mayoral and R. Arenal, Springer International Publishing, Cham, 2015, p. 93; (*e*) L. Liu, U. Díaz, R. Arenal, G. Agostini, P. Concepción and A. Corma, *Nat. Mater.*, 2017, **16**, 132.

21 L. Francés-Soriano, S. Gonzalez-Carrero, E. Navarro-Raga, R. E. Galian, M. González-Béjar and J. Pérez-Prieto, *Adv. Funct. Mater.*, 2016, **26**, 5131.